Journal of Medicinal Chemistry
Brief Article

J. Med. Chem. **2011,** *54,* 1091–1095 **1091**
DOI: 10.1021/jm1010463

Convergent Evolution-Guided Design of Antimicrobial Peptides Derived from Influenza A Virus Hemagglutinin†

Shunyi Zhu,*,‡ André Aumelas,§ and Bin Gao‡

‡*Group of Animal Innate Immunity, State Key Laboratory of Integrated Management of Pest Insects and Rodents, Institute of Zoology, Chinese Academy of Sciences, 1 Beichen West Road, Chaoyang District, Beijing 100101, China, and* §*Centre de Biochimie Structurale, Université Montpellier 1 et 2, CNRS UMR5048, INSERM, U554, 29 Rue de Navacelles, 34090, Montpellier, Cedex 9, France*

Received August 12, 2010

Antimicrobial activity and solution structures of four 13-amino acid peptides derived from the fusion domain of viral hemagglutinin proteins are presented. The results show that carboxyl-terminal amidation is a key factor to switch a viral fusion domain-derived sequence into an antimicrobial peptide. Optimization of amphiphilic balance on the amidated analogue largely improves efficacy and enlarges antimicrobial spectra of these peptides. Our work indicates that viral fusion domains have potential to be engineered into potent antimicrobial peptides.

Introduction

Antibiotic resistance is a worldwide public health problem, and thus, there is an urgent need to discover alternative therapeutics for infectious diseases caused by various pathogenic microorganisms.[1] As naturally occurring effectors of innate immunity, antimicrobial peptides (AMPs[a]) can rapidly kill pathogens through unique modes of action that prevent or delay evolution of microbial resistance to these peptides.[2] Therefore, AMPs are emerging as attractive candidates for development of new type of anti-infective agents.[3] α-Helical AMPs (α-AMPs) are a diverse group of membrane-active molecules ubiquitously distributed in nature.[2,4] These molecules fold into an amphipathic α-helical conformation when binding to microbial membranes, in which cationic amino acids are spatially segregated to one side of the helix and hydrophobic residues on the opposite surface.[2] α-AMPs generally display potent activity against a broad spectrum of bacteria, fungi, protozoa, and viruses. Several examples include cecropins and mellitin from insects, magainin and temporins from frogs, and LL-37, an AMP of 37 amino acids derived from the human cationic antimicrobial protein 18 (hCAP18).[5]

Meucin-13 is a newly identified α-AMP of 13 amino acids from the scorpion *Mesobuthus eupeus*, which inhibits the growth of various microorganisms with high efficiency.[4] Our initial study showed that meucin-13 shares high sequence and structural similarities to the membrane structure of the "fusion domain" (FD) (also called "fusion peptide") of the hemagglutinin (HA) of influenza virus.[4] FD refers to a moderately hydrophobic sequence of approximately 20 amino acids that can adopt an α-helical conformation in a membrane environment and insert into membranes of infected cells to mediate the viral and the host cell membrane fusion.[6] Similarity in sequence, structure, and functional features suggests convergent evolution could have occurred between α-AMPs and viral FDs.[4]

In this work, we exploit functional significance of such convergent evolution by structural and functional evaluation of a synthetic 13-amino acid peptide derived from the FD (named HA-FD-13) and its three analogues. Our results strengthen functional convergence between linear α-helical AMPs and viral FDs and have implications into the development of new AMPs from viral FD-derived sequences.

Results

Molecular Design of Viral FD-Derived Peptides. The FD derived from influenza A H3N2 hemagglutinin (HA) (Swiss-Prot accession number Q6PP25) was chosen as the molecular template for our design. This FD is composed of 19 residues in which 13 show 54−69% sequence identity with meucin-13 depending upon different virus strains.[4] In addition to sequence similarity, the helical wheel projections of meucin-13 and the influenza A/H3N2 HA-FD are also highly similar, both having identical hydrophilic surface comprising residues Gly3, Gly7, Lys10, and Asn11. Of nine residues composed of the hydrophobic surface, four are different, which include three conservative replacements (Leu8Phe, Leu9Ile, and Phe13Trp) and one side chain feature difference (Ile12Gly) (Figure 1A).

To evaluate potential antimicrobial function of viral FDs, we designed and chemically synthesized four peptides based on the influenza A H3N2 HA-FD in reference to meucin-13 sequence, in which two parameters associated with antimicrobial activity were considered: one is C-terminal amidation and the other is amphiphilic balance (Figure 1B). One synthetic peptide, which we named HA-FD-13, is the core region of the FD (GIFGAIAGFIKNGWEGMVD, shown underlined), and three analogues of HA-FD-13 include HA-FD-13a

†The coordinates of HA-FD-13_{aG12I} have been deposited in the Protein Data Bank (http://www.rcsb.org/) under accession code 2L24.

*To whom correspondence should be addressed. Phone: +86 010 64807112. Fax: +86 010 64807099. E-mail: Zhusy@ioz.ac.cn.

[a] Abbreviations: AMP, antimicrobial peptides; HA-FD, hemagglutinin-fusion domain; HPLC, high performance liquid chromatography; MALDI-TOF MS, matrix-assisted laser desorption/ionization time-of-flight mass spectrometry; NMR, nuclear magnetic resonance; t_R, retention time; TFE, trifluoroethanol.

Published on Web 01/11/2011

(the amidated peptide), HA-FD-13$_{G12I}$ (an optimized peptide with one point mutation (G12I) to improve amphiphilic balance), and HA-FD-13$_{aG12I}$ (the amidated peptide of HA-FD-13$_{G12I}$). Overall, these peptides carry one to two net positive charges.

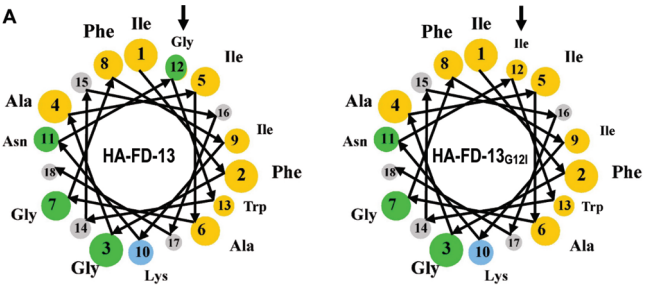

Figure 1. Molecular design of AMPs from the influenza A/H3N2 HA-FD. (A) Helical wheel projections of HA-FD-13[4] and HA-FD-13$_{G12I}$, prepared from http://cti.itc.virginia.edu/, illustrating the hydrophilic and hydrophobic faces of the peptides along the axis of a putative α-helix. Color code for amino acids are as follows: yellow (hydrophobic); green (hydrophilic); blue (basic). The mutated residue at site 12 is indicated by an arrow. (B) Sequence alignment of mucin-13 and HA-FD-derived peptides. Nonidentical residues between meucin-13 and influenza A/H3N2 HA-FD are in red.

Table 1. Properties of HA-FD-13 and Its Mutants

	MW calcd (measd)	net charge	t_R [a]
HA-FD-13	1393.7 (1393.1)	+1	26.1
HA-FD-13$_a$	1392.7 (1392.6)	+2	25.0
HA-FD-13$_{G12I}$	1449.8 (1450.0)	+1	28.5
HA-FD-13$_{aG12I}$	1448.8 (1449.2)	+2	29.0

[a] t_R: retention time (min).

All four peptides were chemically synthesized and characterized by analytic RP-HPLC and MALDI-TOF MS (Table 1). From the RP-HPLC profile, we found that the C-terminal amidation of HA-FD-13 resulted in an increase of polarity, as identified by the retention time (t_R) change from 26.1 to 25.0 min, while the mutation G12I led to more hydrophobicity with t_R from 26.1 to 28.5 min. However, the C-terminal amidation of HA-FD-13$_{G12I}$ led to slight increase rather than decrease of hydrophobicity, as identified by elution at 29.0 min (Table 1).

Antimicrobial Activity of HA-FD and Its Analogues. By using the inhibition zone assay,[7] we evaluated the antimicrobial activity of all four synthetic peptides on three Gram-positive bacteria, nine Gram-negative bacteria, one fungus, and one yeast. Lethal concentrations (C_L) of these peptides are shown in Table 2. The most remarkable features of these viral FD-derived peptides can be extracted as follows: (1) The wild-type of FD (HA-FD-13) only slightly inhibited the growth of *Bacillus* sp. DM-1 with a C_L of 50 μM whereas the mutant HA-FD-13$_{G12I}$ did not enhance the antimicrobial activity of HA-FD-13, indicating that the single mutation to optimize the amphiphilic balance of HA-FD-13 did not have a functional consequence. (2) Relative to HA-FD-13 that carries a C-terminal acid, HA-FD-13a exhibited a 9-fold increase in antibacterial potency on *Bacillus* sp. DM-1 and it also became active on the other four microbial strains (*M. luteus*, *S. marcescens*, *Klebsiella* sp. F51-1-2, and *S. cerevisiae*) that were initially resistant to HA-FD-13. (3) HA-FD-13$_{aG12I}$ showed a wider antimicrobial spectrum and inhibited all microbial strains used here. Remarkably, in comparison with the wild-type peptide, HA-FD-13$_{aG12I}$ displays a 23-fold increase in antibacterial potency on *Bacillus* sp. DM-1. All these data suggest a crucial role of C-terminal amidation in a perfectly amphipathic α-AMPs. (4) Overall, HA-FD-13$_{aG12I}$ shows lower antimicrobial activity than meucin-13;[4] however, this FD-derived peptide evolves the ability to target two Gram-negative bacteria (*Pseudomonas aeruginosa* and *Serratia marcescens*) which were not inhibited by meucin-13. Activity of HA-FD-13$_{aG12I}$ against Gram-negative strains is striking. Moreover, this peptide has approximately 10-fold

Table 2. Antimicrobial Activity of HA-FD-13 and Its Mutants[a]

	HA-FD-13	HA-FD-13$_a$	HA-FD-13$_{G12I}$	HA-FD-13$_{aG12I}$	Meucin-13
			Gram-Positive Bacterium		
Bacillus megaterium	NA	NA	NA	14.10	0.25[b]
Micrococcus luteus	NA	14.10	NA	5.95	2.90[b]
Bacillus sp. DM-1	49.93	5.36	49.93	2.16	2.00[b]
			Gram-Negative Bacterium		
Agrobacterium tumefaciens	NA	NA	NA	20.79	11.80[b]
Pseudomonas aeruginosa	NA	NA	NA	31.55	NA
Salmonella typhimurium	NA	NA	NA	> 100	> 50[b]
Serratia marcescens	NA	> 100	NA	19.25	NA
Shewanella oneidensis	NA	NA	NA	76.98	6.20[b]
Stenotrophomonas sp. YC-1	NA	NA	NA	76.98	6.20[b]
Stenotrophomonus sp. LZ-1	NA	NA	NA	> 100	ND
Klebsiella sp. F51-1-2	NA	> 100	NA	23.81	ND
Pseudomonas putida	NA	NA	NA	9.78	ND
			Fungus		
Geotrichum candidum	NA	NA	NA	5.36	> 50[b]
			Yeast		
Saccharomyces cerevisiae	NA	83.26	NA	28.29	18.30[b]

[a] Lethal concentration (C_L) values are expressed as the concentration of peptides (μM) just sufficient to inhibit growth of the microorganism tested. "NA" means no activity at all concentrations of peptides used here. "ND" means the activity was not determined. [b] Data are derived from ref 4.

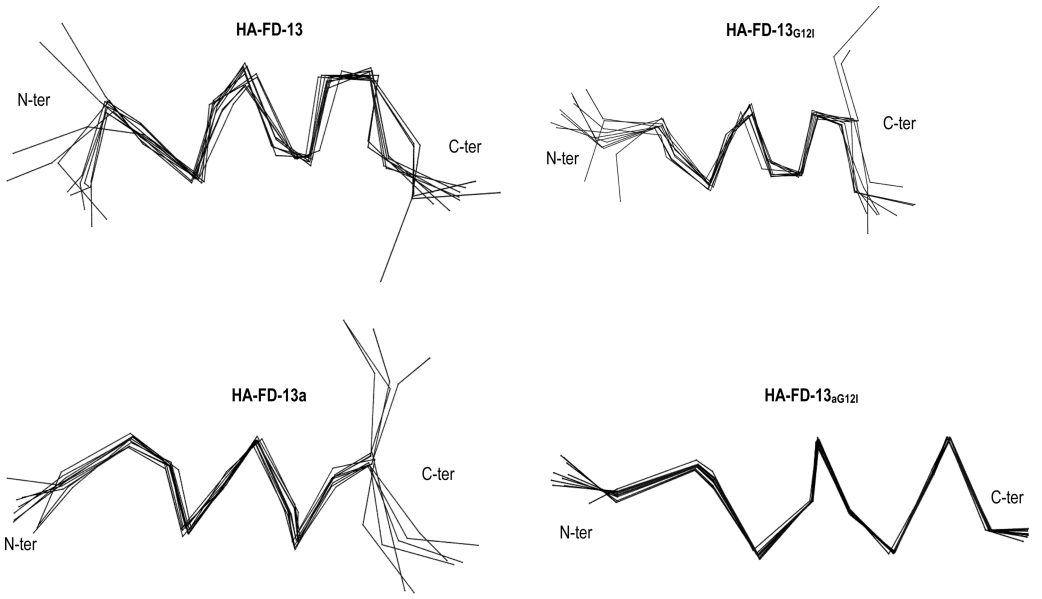

Figure 2. A family of ten conformers of four viral FD-derived peptides, as determined in the presence of 40% of TFE-d_2. The 3−11 backbone atoms were used for the superimposition.

potency compared with meucin-13 on *Geotrichum candidum*, a yeast-like filamentous fungus (Table 2).

To investigate whether these viral FD-derived peptides have the ability to disrupt microbial membranes, we chose HA-FD-13$_{aG12I}$ as a representative to evaluate its effect of membrane permeabilization on *Bacillus* sp. DM-1 using the DNA-binding fluorescent dye propidium iodide (PI).[8] We found that PI only entered peptide-treated bacterial cells (Figure S1), supporting its membranolytic action mode that is similar to that of meucin-13. At 50 μM, HA-FD-13$_{aG12I}$ led to 24.1% hemolysis on fresh mouse blood cells, whereas meucin-13 resulted in 64.7% hemolysis.

NMR Structures of FP-Derived Peptides. In the ^{1}H NMR spectra of HA-FD-13, HA-FD-13a, and HA-FD-13$_{aG12I}$ recorded in water at 22 °C, all amide signals are gathered in the 8.6−8.5 to 7.8−7.6 ppm range and medium- and long-range NOEs are lacking, which both indicate that these peptides are essentially unstructured in water (data not shown). Since HA-FD-13$_{G12I}$ slowly aggregated in water several hours after the sample preparation, which is possibly due to enhanced hydrophobic character after G12I mutation, the study of its amide signals was not carried out in water. However, the addition of 40% TFE-d_2 produced a significant effect on the ^{1}H NMR spectra of all four peptides, as identified by their amide signals upfield shifted in the 8.1−8.3 to 7.5−7.4 ppm range and less spread (0.8−0.7 ppm). The chemical shift deviations are reported in Figure S2. When compared with statistical chemical shift values, the deviations observed clearly support the helical structure for the four peptides. The enhancement of the helical structure content is confirmed by NOESY spectra which display several successive d_{NN} NOEs of strong intensity.

To calculate the solution structures of the four peptides, we used NMR-derived constraints determined in the presence of 40% TFE-d_2 a solvent mixture commonly used to mimic a membrane environment. A family of 10 conformers of the four peptides is displayed in Figure 2. The Ramachandran plot indicated that more than 96.3% and 100% of residues were in the most favored and additional allowed regions. The main part of these structures consists of a well-defined helical

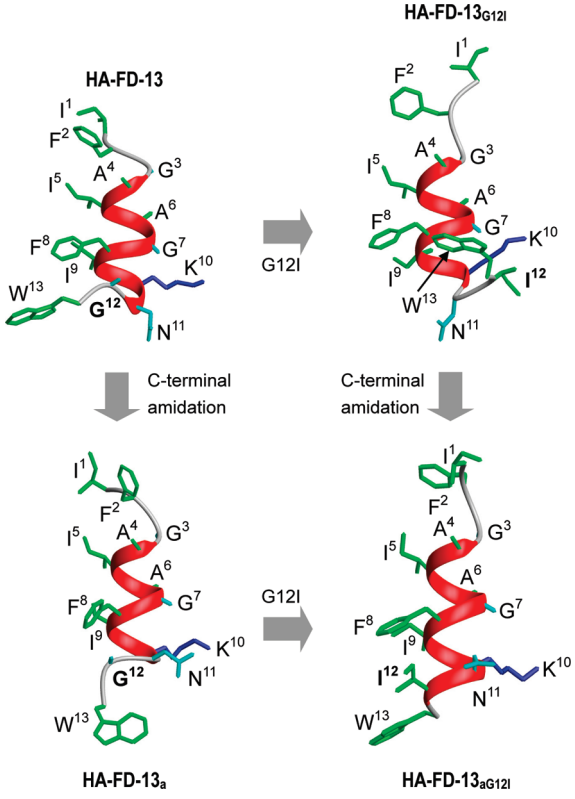

Figure 3. Ribbon structures of four FD-derived peptides in the presence of 40% of TFE-d_2. Amphipathic architecture is highlighted, where hydrophobic, basic, and hydrophilic residues are colored in green, blue, and cyan, respectively.

structure, spanning A4-K10 residues (Figure 3). The C-terminal amidation appears to have some effects on the conformation of the peptides, as identified by structural superimposition that shows smaller rmsd values for the two amide derivatives than their respective nonamidated peptides (i.e., 0.44 ± 0.34 Å for HA-FD-13$_a$ and 0.02 ± 0.01 Å for HA-FD-13$_{aG12I}$). Relative to the nonamidated peptides, the number of H-bonds

Table 3. Activity-Related Structural Features of Viral FD-Derived AMPs[a]

	HA-FD-13	HA-FD-13$_a$	HA-FD-13$_{G12I}$	HA-FD-13$_{aG12I}$
H-bond				
[A^6]HN−O[G^3]	−	+	+	−
[G^7]HN−O[G^3]	−	+	+	+
[F^8]HN−O[A^4]	+	+	+	+
[I^9]HN−O[I^5]	+	+	+	+
[K^{10}]HN−O[A^6]	+	+	+	+
[N^{11}]HN−O[G^7]	+	+	−	+
[I^{12}]HN−O[F^8]	−	−	−	+
[W^{13}]HN−O[I^9]	−	−	−	+
helical region	G^3-K^{10}	G^3-K^{10}	A^4-K^{10}	A^4-K^{12}
C_L[b]	49.93	5.36	49.93	2.16

[a] H-bonds and α-helical regions of these peptides were defined by MOLMOL and STRIDE programs, respectively. [b] Lethal concentrations on *Bacillus* sp. DM-1.

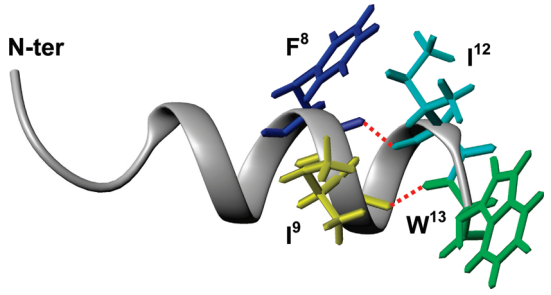

Figure 4. Ribbon structure of HA-FD-13$_{aG12I}$, in which the two additional H-bonds ([I^{12}]HN−O[F^8] and [W^{13}]HN−O[I^9]) are indicated by red dotted lines.

increases in the amidated analogue (Table 3). For example, HA-FD-13 only has four H-bonds whereas HA-FD-13a has six H-bonds. HA-FD-13$_{G12I}$ has five bonds, whereas HA-FD-13$_{aG12I}$ has seven H-bonds. Remarkably, two unique bonds ([I^{12}]HN−O[F^8] and [W^{13}]HN−O[I^9]) are only present in HA-FD-13$_{aG12I}$ (Figure 4), supporting their role in stabilizing the helical conformation and expressing the antimicrobial activity. Activity enhancement by C-terminal amidation have been also observed in several AMPs, such as dermaseptin S3,[9] decoralin,[10] and Hb33-61,[11] their antimicrobial activities were also enhanced after C-terminal amidation.

Besides the role in increasing the helical content, C-terminal amidation also results in addition of one positive charge, which likely ensures electrostatic interactions and accumulation of peptides on the polyanionic microbial membranes surfaces.

Discussion

Previous studies have indicated that some viral FDs possess characteristics similar to α-AMPs,[4,12,13] which mainly include the preference of aliphatic amino acids (e.g., Ala, Gly, Ile) and an overall amphiphilic α-helical architecture. Such similarity could be a consequence of structural and functional convergence because disrupting or disturbing lipid bilayers of cellular membranes is their common action mode. In this case, a short α-helical scaffold carrying these aliphatic residues is required to support interactions between peptides and membranes. These observations hint at a possible antimicrobial function of viral FDs. However, such a function for these viral FDs is not yet evaluated. The work presented here for the first time confirms the potential of viral FDs in exploring potent AMPs.

Our results demonstrate that although the viral FD-derived peptide itself has very weak antimicrobial activity, minor sequence modifications are sufficient to obtain a potent AMP. We found that C-terminal amidation alone contributes to the increase of biological activity of the viral FD (HA-FD-13) due to addition of one positive charge and more helical content. Further modification to optimize the amphipathicity of this peptide largely improves its potency and range of antimicrobial activity. This finding highlights the importance of C-terminal amidation in combination with amphiphilic balance in the emergence of antimicrobial function of the FD-derived peptide. In such a case, an effectively structural context may more facilitate the positive charges of HA-FD-13$_{aG12I}$ to interact with anionic microbial membranes. This explanation is consistent with the observation that the two amidated peptides (HA-FD-13a and HA-FD-13$_{aG12I}$) have similar charges but different activities because of differences in their helicity (H-bond pattern) and amphipathicity. A cationic α-helical peptide, named meucin-24,[14] provides support for this assumption. This peptide contains 24 amino acids and share overall structural and sequence similarity to the classical frog-derived AMPs, magainins; however, it lacks antibacterial and antifungal activities because of its helical conformation being unable to support a rational location of the positively charged residues.

Further mutagenesis experiments are required to find a balance between net cationic charge and amphiphilic helicity important for biological activity/selectivity of these new AMPs, which will be valuable in guiding the design of more potent molecules with therapeutic potential.

Experimental Section

Antimicrobial Assays. HA-FD-13 and its analogues were synthesized by Xi'an Huachen Bio-Technology Co., Ltd. (Xian, China), which have more than 95% purity, as confirmed by RP-HPLC and MALDI-TOF MS.

Inhibition zone assays were used to determine antimicrobial activity of these synthetic peptides, which were carried out according to the literature.[7] Lethal concentration (C_L) values are calculated from a plot of d^2 against $\log n$, where d is the diameter (in cm) and n is the amount of sample applied in the well (in nmol). The plot is linear, and thus, C_L can be calculated from the slope (k) and the intercept (m) of this plot. The formula used here is $C_L = 2.93/(ak10^{m/k})$, where a is the thickness of the bacterial plate and C_L is in μM.[7]

Membrane Permeabilization Assays. Membrane permeabilization of HA-FD-13$_{aG12I}$ on Bacillus sp. DM-1 was carried out according to the method of Amino et al.[8] with some modifications. In brief, 100 μL of cell culture (OD_{600} = 0.5) was taken and the peptide was added to a final concentration of 10 μM. After 30 min of incubation, the fluorescent dye propidium iodide (PI) was added to a final concentration of 10 μg/mL and cells were photographed in a phase contrast/fluorescence microscope after being washed 3 times with PBS buffer.

Hemolytic Assays. Hemolytic activity of HA-FD-13$_{aG12I}$ against fresh mouse blood cells was evaluated according to the standard method.[15] Absorbance was measured at 570 nm. 100% hemolysis was obtained in the presence of 1% Triton X-100.

NMR Spectroscopy. For each peptide, two 1.5−2.0 mM samples were prepared, one in a 95:5 (v/v) mixture of H_2O/D_2O and the other in a 60:40 (v/v) mixture of H_2O/trifluoroethanol-d_2 (TFE-d_2). Proton chemical shifts are expressed with respect to sodium 4,4-dimethyl-4-silapentane-1-sulfonate according to the IUPAC recommendations. All ^{1}H NMR experiments were recorded at 22 °C on a Bruker Avance 600 spectrometer equipped with a triple resonance cryoprobe. In all experiments, the carrier frequency was set at the water frequency at the center of the spectrum. Double-quantum-filtered correlation spectroscopy

(DQF-COSY),[16] z-filtered total-correlation spectroscopy (z-TOCSY),[17] and nuclear Overhauser effect spectroscopy (NOESY)[18] spectra were acquired in the phase-sensitive mode, using the States-TPPI method.[19] The water resonance was suppressed by the WATERGATE method,[20] except for DQF-COSY spectra, for which low-power irradiation was used. z-TOCSY spectra were obtained with a mixing time of 80 ms and NOESY spectra with a mixing time of 250 ms. The study in the presence of TFE-d_2 was carried out at 22 °C by recording a similar set of experiments as in water. Data were processed with XWINNMR software. Full sequential assignment was achieved using the general strategy.

Calculation of Structures. NMR-derived constraints measured on the NOESY spectrum recorded in the presence of 40% TFE-d_2 were converted into interproton upper distance limits of 2.5, 3.0, 4.0, and 5.0 Å for strong, medium, weak, and very weak intensities, respectively. As no stereospecific assignment was possible for the methyl and methylene protons, pseudoatoms were used instead, after appropriate corrections of the constraints. The ϕ angle restraints were estimated from the $^3J_{NH-CH}$ coupling constants, and the χ_1 angle restraints were derived from the combined analysis of the $^3J_{H\alpha\text{-}H\beta\beta'}$ coupling constants and intraresidue NOEs. For the calculation of 3D structures, distance and dihedral angle restraints were input into DYANA, a program using simulated annealing combined with molecular dynamics in torsion angle space.[21] In the first stage of the calculation, an initial set of 20 structures was generated from a template structure with randomized Ψ, Φ dihedral angles and extended side chains. In preliminary calculations, hydrogen bonds were not used as a restraint. Hydrogen bonds were considered to be present if the distance between heavy atoms was less than 3.5 Å and the donor−hydrogen−acceptor angle was greater than 120°.

Finally, we used 79 and 8 (HA-FD-13), 85 and 6 (HA-FD-13a), 90 and 6 (HA-FD-13_{G12I}) and 97 and 8 (HA-FD-13_{aG12I}) NOE-derived distances and dihedral constraints to calculate the solution structures of the four peptides. Final calculations were made for 100 conformers, and the resulting 10 structures with minimal restraint violations (no violation of >0.3 Å) were analyzed with INSIGHT 97 (Molecular Simulation Inc., San Diego, CA). Ramachandran analysis was performed with PROCHECK.[22] The limits of the secondary structure elements were determined with STRIDE.[23]

Acknowledgment. This work was supported by the National Natural Science Foundation of China (Grants 30730015 and 30921006) and the National Basic Research Program of China (Grant 2010CB945300).

Supporting Information Available: Results of membrane permeabilization assays (Figure S1) and chemical shift deviations (Figure S2). This material is available free of charge via the Internet at http://pubs.acs.org.

References

(1) Levy, S. B.; Marshall, B. Antibacterial resistance worldwide: causes, challenges and responses. *Nat Med.* **2004**, *10* (12, Suppl.), S122–S129.
(2) Zasloff, M. Antimicrobial peptides of multicellular organisms. *Nature* **2002**, *415*, 389–395.
(3) Hancock, R. E. W.; Sahl, H.-G. Antimicrobial and host-defense peptides as new anti-infective therapeutic strategies. *Nat. Biotechnol.* **2006**, *24*, 1551–1557.
(4) Gao, B.; Sherman, P.; Luo, L.; Bowie, J.; Zhu, S. Structural and functional characterization of two genetically related meucin peptides highlights evolutionary divergence and convergence in antimicrobial peptides. *FASEB J.* **2009**, *23*, 1230–1245.
(5) Bulet, P.; Stöcklin, R.; Menin, L. Anti-microbial peptides: from invertebrates to vertebrates. *Immunol. Rev.* **2004**, *198*, 169–184.
(6) Tamm, L. K. Hypothesis: spring-loaded boomerang mechanism of influenza hemagglutinin-mediated membrane fusion. *Biochim. Biophys. Acta* **2003**, *1614*, 14–23.
(7) Hultmark, D. Quantification of Antimicrobial Activity, Using the Inhibition-Zone Assay. In *Techniques in Insect Immunology*; Wiesner, A., Dumphy, A. G., Marmaras, V. J., Morishima, I., Sugumaran, M., Yamakawa, M., Eds.; SOS Publications: Fair Haven, NJ, 1998; pp 103−107.
(8) Amino, R.; Martins, R. M.; Procopio, J.; Hirata, I. Y.; Juliano, M. A.; Schenkman, S. Trialysin, a novel poreforming protein from saliva of hematophagous insects activated by limited proteolysis. *J. Biol. Chem.* **2002**, *277*, 6207–6213.
(9) Shalev, D. E.; Mor, A.; Kustanovich, I. Structural consequences of carboxyamidation of dermaseptin S3. *Biochemistry* **2002**, *41*, 7312–7317.
(10) Konno, K.; Rangel, M.; Oliveira, J. S.; Dos Santos Cabrera, M. P.; Fontana, R.; Hirata, I. Y.; Hide, I.; Nakata, Y.; Mori, K.; Kawano, M.; Fuchino, H.; Sekita, S.; Neto, J. R. Decoralin, a novel linear cationic alpha-helical peptide from the venom of the solitary eumenine wasp *Oreumenes decoratus*. *Peptides* **2007**, *28*, 2320–2327.
(11) Machado, A.; Sforça, M. L.; Miranda, A.; Daffre, S.; Pertinhez, T. A.; Spisni, A.; Miranda, M. T. Truncation of amidated fragment 33−61 of bovine alpha-hemoglobin: effects on the structure and anticandidal activity. *Biopolymers* **2007**, *88*, 413–426.
(12) Han, X.; Kang, W. Sequence analysis and membrane partitioning energies of α-helical antimicrobial peptides. *Bioinformatics* **2004**, *20*, 970–973.
(13) Joanne, P.; Nicolas, P.; El Amri, C. Antimicrobial peptides and viral fusion peptides: how different they are? *Protein Pept. Lett.* **2009**, *16*, 743–750.
(14) Gao, B.; Xu, J.; Lanz-Mendoza, H.; del Carmen Rodriguez, M.; Hernández-Rivas, R.; Du, W.; Zhu, S. Characterization of two linear cationic antimalarial peptides in the scorpion *Mesobuthus eupeus*. *Biochimie* **2010**, *92*, 350–359.
(15) Tossi, A.; Scocchi, M.; Zanetii, M.; Gennaro, R.; Storici, P.; Romeo, D. An Approach Combining Rapid cDNA Amplification and Chemical Synthesis for Identification of Novel, Cathelicidin-Derived Antimicrobial Peptides. In *Antibacterial Peptide Protocols*; Shafer, W. M., Ed.; Humana Press: Tokowa, NJ, 1997; pp 133−150.
(16) Derome, A. E.; Williamson, M. P. Rapid-pulsing artifacts in doube-quantum-filtered COSY. *J. Magn. Reson.* **1990**, *88*, 177–185.
(17) Bax, A.; Davis, G. D. MLEV-17-based two-dimensional homonuclear magnetization transfer spectroscopy. *J. Magn. Reson.* **1985**, *65*, 355–360.
(18) Macura, S.; Huang, Y.; Sutter, D.; Ernst, R. R. Two-dimensional chemical exchange and cross-relaxation spectroscopy of coupled nuclear spins. *J. Magn. Reson.* **1981**, *43*, 259–281.
(19) Marion, D.; Ikura, M.; Tschudin, R.; Bax, A. Rapid recording of 2D NMR spectra without phase cycling. Application to the study of hydrogen exchange in proteins. *J. Magn. Reson.* **1989**, *85*, 393–399.
(20) Piotto, M.; Saudek, V.; Sklenar, V. Gradient-tailored excitation for single-quantum NMR spectroscopy of aqueous solutions. *J. Biomol. NMR* **1992**, *2*, 661–665.
(21) Guntert, P.; Mumenthaler, C.; Wuthrich, K. Torsion angle dynamics for NMR structure calculation with the new program DYANA. *J. Mol. Biol.* **1997**, *273*, 283–298.
(22) Laskowski, R. A.; Rullmannn, J. A.; MacArthur, M. W.; Kaptein, R.; Thornton, J. M. AQUA and PROCHECK-NMR: programs for checking the quality of protein structures solved by NMR. *J. Biomol. NMR* **1996**, *8*, 477–486.
(23) Frishman, D.; Argos, P. Knowledge-based protein secondary structure assignment. *Proteins* **1995**, *23*, 566–579.